Derivation of mean dose tolerances for new fractionation schemes and treatment modalities

Perkó, Zoltán ; Bortfeld, Thomas R ; Hong, Theodore S ; Wolfgang, John ; Unkelbach, Jan

Abstract: Avoiding toxicities in radiotherapy requires the knowledge of tolerable organ doses. For new, experimental fractionation schemes (e.g. hypofractionation) these are typically derived from traditional schedules using the Biologically Effective Dose (BED) model. In this report we investigate the difficulties of establishing mean dose tolerances that arise since the mean BED depends on the entire spatial dose distribution, rather than on the dose level alone.13; 13; Methods: A formula has been derived to establish mean physical dose constraints such that they are mean BED equivalent to a reference treatment scheme. This formula constitutes a modified BED equation where the influence of the spatial dose distribution is summarized in a single parameter, the dose shape factor. To quantify effects we analyzed 24 liver cancer patients for whom both proton and photon IMRT treatment plans were available.13; 13; Results: The results show that the standard BED equation - neglecting the spatial dose distribution - can overestimate mean dose tolerances for hypofractionated treatments by up to 20%. The shape difference between photon and proton dose distributions can cause 30-40% differences in mean physical dose for plans having identical mean BEDs. Converting hypofractionated, 5/15-fraction proton doses to mean BED equivalent photon doses in traditional 35-fraction regimens resulted in up to 10 Gy higher doses than applying the standard BED formula. 13; 13; Conclusions: The dose shape effect should be accounted for to avoid overestimation of mean dose tolerances, particularly when estimating constraints for hypofractionated regimens. Additionally, tolerances established for one treatment modality cannot necessarily be applied to other modalities with drastically different dose distributions, such as proton therapy. Last, protons may only allow marginal (5-10%) dose escalation if a fraction-size adjusted organ mean dose is constraining instead of a physical dose.

DOI: https://doi.org/10.1088/1361-6560/aa9836

Derivation of mean dose tolerances for new fractionation schemes and treatment modalities

To cite this article before publication: Zoltán Perkó *et al* 2017 *Phys. Med. Biol.* in press https://doi.org/10.1088/1361-6560/aa9836

Derivation of Mean Dose Tolerances for New Fractionation Schemes and Treatment Modalities

Zoltán Perkó, PhD*[1,2], Thomas Bortfeld, PhD†[1], Theodore Hong, MD‡[1], John Wolfgang, PhD§[1], and Jan Unkelbach, PhD¶[1,3]

[1]Massachusetts General Hospital, Department of Radiation Oncology, Boston, Massachusetts, US.
[2]Currently at Delft University of Technology, Delft, Netherlands.
[3]Currently at University Hospital Zürich, Zürich, Switzerland.

2017.09.12.

Abstract

Purpose: Avoiding toxicities in radiotherapy requires the knowledge of tolerable organ doses. For new, experimental fractionation schemes (e.g. hypofractionation) these are typically derived from traditional schedules using the Biologically Effective Dose (BED) model. In this report we investigate the difficulties of establishing mean dose tolerances that arise since the mean BED depends on the entire spatial dose distribution, rather than on the dose level alone.

Methods: A formula has been derived to establish mean physical dose constraints such that they are mean BED equivalent to a reference treatment scheme. This formula constitutes a modified BED equation where the influence of the spatial dose distribution is summarized in a single parameter, the dose shape factor. To quantify effects we analyzed 24 liver cancer patients for whom both proton and photon IMRT treatment plans were available.

Results: The results show that the standard BED equation - neglecting the spatial dose distribution - can overestimate mean dose tolerances for hypofractionated treatments by up to 20%. The shape difference between photon and proton dose distributions can cause 30-40% differences in mean physical dose for plans having identical mean BEDs. Converting hypofractionated, 5/15-fraction proton doses to mean BED equivalent photon doses in traditional 35-fraction regimens resulted in up to 10 Gy higher doses than applying the standard BED formula.

Conclusions: The dose shape effect should be accounted for to avoid overestimation of mean dose tolerances, particularly when estimating constraints for hypofractionated regimens. Additionally, tolerances established for one treatment modality cannot necessarily be applied to other modalities with drastically

*Corresponding author: z.perko@tudelft.nl
†TBortfeld@mgh.harvard.edu
‡TSHong1@mgh.harvard.edu
§jwolfgang@partners.org
¶Jan.Unkelbach@usz.ch

different dose distributions, such as proton therapy. Last, protons may only allow marginal (5-10%) dose escalation if a fraction-size adjusted organ mean dose is constraining instead of a physical dose.

Keywords: BED, Normal Tissue Tolerance, Proton Therapy, IMRT, Mean Dose Constraints.

1 Introduction

The safe use of radiotherapy requires the knowledge of radiation doses that healthy tissues can tolerate. These dose tolerances are typically obtained from clinical data by correlating dose metrics with the occurrence rates of radiation toxicities. Subsequently, they guide the selection of dose constraints in treatment planning to limit the risk of radiation induced side effects. The most common constraints are maximum dose, mean dose, Dose Volume Histogram (DVH) and generalized Equivalent Uniform Dose (gEUD) constraints [1, 2, 3, 4, 5].

Since the beneficial effects of fractionated radiotherapy have been discovered early on [6, 7, 8, 9, 10, 11], the vast majority of treatments have applied 25-35 fractions with 2 Gy dose per fraction, leading to total target doses of 50 Gy to 70 Gy. This is referred to as the standard fractionation. Consequently, most dose tolerances have been determined for these conventional fractionation schedules. Current trends towards hypofractionation [12, 13, 14, 15] (i.e. the use of fewer fractions with higher dose per fraction) require dose tolerances for such experimental regimens, too. Additionally, the spread of charged particle therapy necessitates establishing dose tolerances for new treatment modalities as well.

Before routine clinical use, dose constraints for a new fractionation scheme (or modality) always have to be validated by outcome data. However, in the initial design of clinical trials testing an experimental treatment schedule, the Biologically Effective Dose (BED) [8, 10, 16, 17] model is often used to derive dose tolerances from established fractionation schemes. The procedure for establishing maximum dose constraints - where only a single dose level is considered - is familiar to practitioners [18, 5, 8, 17, 19, 20, 21]. Our paper focuses on the derivation of mean dose tolerances, where additional difficulties arise. Specifically, we address 3 questions:

- How can mean dose constraints be established for new fractionation schemes using the BED model? Mean organ doses are used to estimate normal tissue complications for several major treatment sites (e.g. liver, lung [22, 23, 24, 25]). Therefore, the derivation of mean dose tolerances in new (hypofractionated) treatment schedules directly affects their safety. Since the mean BED in an organ depends not only on the mean physical dose, but also on the entire, typically inhomogeneous dose distribution, this should be accounted for (Section 3.2).

- Can mean dose constraints established for one modality (e.g. 3DCRT or IMRT) be applied one-to-one to other modalities (e.g. VMAT, protons)? In clinical trials investigating the efficacy of proton treatments (vs. photons), dose escalation is often done based on the mean physical dose of adjacent healthy organs [26]. However, proton dose distributions are significantly different from photon distributions: for the same mean dose, protons typically emphasize the high dose region and reduce the low dose bath. Consequently, proton plans usually have higher mean BED for the same mean dose, making it important to study the potential effects of the spatial differences (Section 3.3).

- What is the dose escalation potential of proton therapy vs. photons for the same normal tissue complication probability (NTCP)? Current proton therapy plans often have larger margins around the target structures than state-of-the-art IMRT plans, mainly due to uncertainties in proton range (e.g. a typical 3.5% range uncertainty can translate to a distal margin up to 1 cm [27]). At the same time, adjusting for fractionation with the BED model effects high dose values more than low doses. Consequently the dose escalation potential of proton therapy, as assessed from gEUD based NTCP-models, is expected to decrease when the physical dose is adjusted for fractionation. With the spread of particle therapy treatments aimed at increasing target doses these effects should be investigated (Section 3.5).

2 Methods and Materials

2.1 Biologically Effective Dose Model

To describe fractionation effects we use the standard BED model [8, 10, 16, 17], stating that the biological dose is

$$\mathrm{BED} = Nd\left(1+\frac{d}{\alpha/\beta}\right) = D\left(1+\frac{D}{N\alpha/\beta}\right), \tag{1}$$

where $D = Nd$ is the total dose given in N fractions with dose per fraction d, and α/β represents the fractionation sensitivity of the tissue. Equation 1 is frequently used to guide the derivation of iso-effective doses in experimental fractionation schemes based on established schemes [5, 8, 17, 19, 20]. If an organ-at-risk (OAR) can tolerate a dose D_{ref} in N_{ref} fractions, the tolerance in a new scheme with N_{new} fractions can be obtained by equating the BEDs for the two regimens, i.e. solving

$$D_{\mathrm{new}}\left(1+\frac{D_{\mathrm{new}}}{N_{\mathrm{new}}\alpha/\beta}\right) = D_{\mathrm{ref}}\left(1+\frac{D_{\mathrm{ref}}}{N_{\mathrm{ref}}\alpha/\beta}\right) \tag{2}$$

for the new dose tolerance D_{new}. The solution is

$$D_{\mathrm{new}} = \frac{1}{2}\left[\sqrt{\left(N_{\mathrm{new}}\alpha/\beta\right)^2 + 4D_{\mathrm{ref}}\left(N_{\mathrm{new}}\alpha/\beta + D_{\mathrm{ref}}\frac{N_{\mathrm{new}}}{N_{\mathrm{ref}}}\right)} - N_{\mathrm{new}}\alpha/\beta\right]. \tag{3}$$

Equation 3 is equivalent to the well-known Withers iso-effect formula [21], except here we use the total dose and the number of fractions as variables instead of the total dose and the dose per fraction. Traditionally, the Withers formula has been used to derive maximum dose constraints for serial OARs located within or near the target volume. In this case the reference dose D_{ref} is given by the prescription dose and it is assumed that the OAR receives the same dose. Therefore, as also pointed out in [18], this approach implicitly assumes that the iso-effect is calculated for a serial organ receiving the same dose in the same number of fractions as the tumor.

2.2 Mean BED vs. BED of the Mean

Not every OAR can however be considered serial and radiation induced side effects not only depend on the maximum dose: for different organs various Dose Volume Histogram (DVH) metrics were found to be predictive of normal tissue damage [28, 5]. Consequently, NTCP models typically include DVH reduction methods (e.g. gEUD or effective volume) using a volume parameter n to describe the "volume effect" of organs [29, 1, 30], with n being close to zero when the effect is small (in serial organs) and around unity when the effect is large (in parallel organs). The exact value of the volume parameter is subject to considerable uncertainty, however, for several OARs it has been found to be sufficiently close to 1 [31, 24] such that simply the mean dose could be considered predictive of radiation damage.

In clinical radiotherapy practice therefore mean dose tolerances are still commonly employed in treatment planning for organs with parallel structure (e.g. lung, liver [22, 23, 24]). Hence it is desirable to be able to use the BED model to derive mean dose tolerances in experimental fractionation schemes from established ones. The difficulty arises from the fact that the true mean BED of an inhomogeneous dose distribution is not the same as the BED corresponding to the mean physical dose of that distribution. Introducing the voxel doses D_i (and for later use the dose vector $\boldsymbol{D} = (D_1, D_2, ..., D_M)$, where M is the number of voxels), the mean BED can be calculated using the mean physical dose $D_{\mathrm{mean}} = 1/M\sum_{i=1}^{M} D_i$ as:

$$\mathrm{BED}_{\mathrm{mean}} = \frac{1}{M}\sum_{i=1}^{M}\mathrm{BED}_i = \frac{1}{M}\sum_{i=1}^{M} D_i\left(1+D_i/\left(N\alpha/\beta\right)\right) = D_{\mathrm{mean}}\left(1+\frac{1}{D_{\mathrm{mean}}}\frac{\frac{1}{M}\sum_{i=1}^{M}D_i^2}{N\alpha/\beta}\right)$$

$$= D_{\mathrm{mean}}\left(1+\frac{D_{\mathrm{mean}}}{N\alpha/\beta}\frac{\frac{1}{M}\sum_{i=1}^{M}D_i^2}{\left(\frac{1}{M}\sum_{i=1}^{M}D_i\right)^2}\right) = D_{\mathrm{mean}}\left(1+\frac{D_{\mathrm{mean}}}{N\alpha/\beta}\frac{M\sum_{i=1}^{M}D_i^2}{\left(\sum_{i=1}^{M}D_i\right)^2}\right). \tag{4}$$

Equation 4 reveals that the mean BED is not only defined by the mean physical dose and the fractionation scheme, but also by the spatial distribution of the dose. The effect of the dose distribution can be summarized by a single dimensionless parameter, the dose shape factor

$$\varphi = \frac{M \sum_{i=1}^{M} D_i^2}{\left(\sum_{i=1}^{M} D_i\right)^2}. \tag{5}$$

The appendix of [18] gives a practically identical derivation for Equation 4, but calls the dose shape factor of Equation 5 the "dose heterogeneity factor", and implicitly [32] also makes use of this formulation. In essence, the dose shape factor provides a practical, straightforward insight into the effect of the dose distribution on the mean BED (however, it "only" accounts for the shape, and not for example for organ structure or heterogeneities in radiobiological properties, etc.).

Using Equation 5 allows the mean BED to be calculated as

$$\mathrm{BED}_{\mathrm{mean}} = D_{\mathrm{mean}} \left(1 + \frac{D_{\mathrm{mean}}}{N\alpha/\beta}\varphi\right).$$

Therefore, to obtain mean dose tolerances D_{new} for a treatment modality characterized by φ_{new}, based on a reference modality with dose shape factor φ_{ref} and mean dose tolerance D_{ref}, one has to solve

$$D_{\mathrm{new}} \left(1 + \frac{D_{\mathrm{new}}}{N_{\mathrm{new}}\alpha/\beta}\varphi_{\mathrm{new}}\right) = D_{\mathrm{ref}} \left(1 + \frac{D_{\mathrm{ref}}}{N_{\mathrm{ref}}\alpha/\beta}\varphi_{\mathrm{ref}}\right) \tag{6}$$

for D_{new} (instead of Equation 2). The solution is

$$D_{\mathrm{new}} = \frac{1}{2}\left[\sqrt{\left(\frac{N_{\mathrm{new}}\alpha/\beta}{\varphi_{new}}\right)^2 + 4D_{\mathrm{ref}}\left(\frac{N_{\mathrm{new}}\alpha/\beta}{\varphi_{\mathrm{new}}} + D_{ref}\frac{\varphi_{\mathrm{ref}}}{\varphi_{\mathrm{new}}}\frac{N_{\mathrm{new}}}{N_{\mathrm{ref}}}\right)} - \frac{N_{\mathrm{new}}\alpha/\beta}{\varphi_{\mathrm{new}}}\right]. \tag{7}$$

There are 3 important aspects regarding the impact of the dose shape factor on the mean BED:

- The dose shape factor is never smaller than unity, i.e. $\varphi \geq 1$. Therefore the mean BED is always bigger than the simple BED equivalent of the mean physical dose ($\varphi = 1$ only holds for completely homogeneous distribution).
- The dose shape factor and the mean BED both increase with the variance of the spatial dose distribution[1] [18]. This can be seen if we use the variance of the dose distribution, $var\left(\boldsymbol{D}\right) = 1/M \sum_{i=1}^{M} \left(D_i - D_{\mathrm{mean}}\right)^2$, to rewrite Equation 5 as

  $$\varphi = \frac{1}{D_{\mathrm{mean}}}\frac{\sum_{i=1}^{M} D_i^2}{\sum_{i=1}^{M} D_i} = \frac{1}{D_{\mathrm{mean}}}\left(D_{\mathrm{mean}} + \frac{var\left(\boldsymbol{D}\right)}{D_{\mathrm{mean}}}\right).$$

  Higher variance in the dose distribution therefore leads to higher φ and mean BED as well.
- Two treatments with identical mean physical doses $D^1_{\mathrm{mean}} = D^2_{\mathrm{mean}}$ and fractionation schemes $N^1 = N^2$ are not necessarily equivalent in terms of mean BED. $\mathrm{BED}^1_{\mathrm{mean}} = \mathrm{BED}^2_{\mathrm{mean}}$ only holds if the spatial distributions are also similar, i.e. if $\varphi^1 = \varphi^2$.

2.3 Consistency with gEUD Based NTCP Modelling

Requiring the equivalence of the mean BEDs (Equation 6) is consistent with typical NTCP modelling. This is presented in details in Section A. The main result is that for a majority of NTCP models - including the popular Lyman-Kutcher-Burman model (see Section B) - two dose distributions have the same NTCP if they have identical "generalized Equivalent Uniform Biologically Effective Doses" [33, 18], i.e. if

$$\mathrm{gEUBED}_n\left(\boldsymbol{D}_{\mathrm{new}}, N_{\mathrm{new}}, \alpha/\beta\right) = \mathrm{gEUBED}_n\left(\boldsymbol{D}_{\mathrm{ref}}, N_{\mathrm{ref}}, \alpha/\beta\right). \tag{8}$$

[1] Temporal variance similarly increases the mean BED, see Section 1.1 of the Supplementary Materials (SM).

The "generalized Equivalent Uniform Biologically Effective Dose", denoted by $\mathrm{gEUBED}_n(\boldsymbol{D}, N, \alpha/\beta)$ is simply a generalized Equivalent Uniform Dose calculation $\mathrm{gEUD}_n(\mathbf{BED}(\boldsymbol{D}, N, \alpha/\beta))$ based on the BED distribution $\mathbf{BED}(\boldsymbol{D}, N, \alpha/\beta)$ corresponding to the physical dose distribution $\boldsymbol{D}$ given in N fractions, with fractionation sensitivity α/β, using n as the volume parameter:

$$\mathrm{gEUBED}_n(\boldsymbol{D}, N, \alpha/\beta) = \left(\frac{1}{M}\sum_{i=1}^{M}\mathrm{BED}_i^{1/n}\right)^n = \left[\frac{1}{M}\sum_{i=1}^{M}\left(D_i\left(1+\frac{D_i}{N\alpha/\beta}\right)\right)^{1/n}\right]^n. \quad (9)$$

For $n = 1$ the gEUD is identical to the arithmetic mean and Equation 8 simplifies to Equation 6, which can be solved analytically to yield Equation 7.

We specifically use Equation 8 to study iso-toxic dose escalation. To calculate how a dose distribution $\boldsymbol{D}_{\mathrm{new}}$ can be scaled to a distribution $f \cdot \boldsymbol{D}_{\mathrm{new}}$ such that it leads to the same NTCP as the reference distribution $\boldsymbol{D}_{\mathrm{ref}}$,

$$\mathrm{gEUBED}_n(f \cdot \boldsymbol{D}_{\mathrm{new}}, N_{\mathrm{new}}, \alpha/\beta) = \mathrm{gEUBED}_n(\boldsymbol{D}_{\mathrm{ref}}, N_{\mathrm{ref}}, \alpha/\beta)$$

has to hold. Filling in the formula for calculating the gEUBEDs (Equation 9) for the two dose distributions leads to

$$\left[\frac{1}{M}\sum_{i=1}^{M}\left(f\cdot D_{\mathrm{new},i}\left(1+\frac{f\cdot D_{\mathrm{new},i}}{N_{\mathrm{new}}\alpha/\beta}\right)\right)^{1/n}\right]^n = \left[\frac{1}{M}\sum_{i=1}^{M}\left(D_{\mathrm{ref},i}\left(1+\frac{D_{\mathrm{ref},i}}{N_{\mathrm{ref}}\alpha/\beta}\right)\right)^{1/n}\right]^n. \quad (10)$$

For given dose distributions ($\boldsymbol{D}_{\mathrm{new}}$, $\boldsymbol{D}_{\mathrm{ref}}$), fraction numbers ($N_{\mathrm{new}}$, N_{ref}) and chosen n and α/β values, the only unknown is the scaling factor f. Hence numerically solving Equation 10 for f provides a general method for iso-NTCP based dose escalation.

2.4 Using BED Formulas

The effects of the dose shape factor on the mean BED - detailed in Section 2.2 - have important consequences when iso-effective (i.e. iso-toxic) mean doses are calculated between fractionation schemes and between modalities. We consider 3 scenarios corresponding to special cases of Equation 6:

- Case 1 demonstrates the effects of the dose shape when doses are calculated between fractionation schemes ($N_{\mathrm{new}} \neq N_{\mathrm{ref}}$) for the same irradiation modality ($\varphi_{\mathrm{new}} = \varphi_{\mathrm{ref}}$, Section 3.2).
- Case 2 compares different modalities ($\varphi_{\mathrm{new}} \neq \varphi_{\mathrm{ref}}$) for the same fractionation ($N_{\mathrm{new}} = N_{\mathrm{ref}}$, Section 3.3). We consider photons as the reference (with φ_{ref} being the photon dose shape factor) and calculate the mean dose in photon plans ($D_{\mathrm{ref}} = D_{\mathrm{new}} + \Delta D$) that is mean BED equivalent with proton mean doses D_{new} (with φ_{new} being the proton dose shape factor). The difference $\Delta D = D_{\mathrm{ref}} - D_{\mathrm{new}}$ represents an effective dose difference resulting from the shape difference $\Delta\varphi = \varphi_{\mathrm{new}} - \varphi_{\mathrm{ref}}$.
- Case 3 uses Equation 6 to relate one treatment with dose shape φ_{new}, N_{new} fractions, and mean dose D_{new} to another treatment characterized by φ_{ref}, N_{ref} fractions, and D_{ref} (Section 3.4). Specifically, for a hypofractionated proton treatment with mean dose D_{new} and dose shape factor φ_{new} ($N_{\mathrm{new}} = 5$ or 15), we calculate the mean dose D_{ref} in a conventionally fractionated ($N_{\mathrm{ref}} = 35$) photon plan with dose shape factor φ_{ref}, that would be mean BED equivalent.

Additionally, we study the dose escalation potential of proton therapy vs. photon therapy as assessed by iso-NTCP based dose escalation:

- Case 4 compares the given proton plans $\boldsymbol{D}_{\mathrm{proton}}$ (which were delivered to the patients in $N = 5$ or 15 fractions) to the planned photon plans $\boldsymbol{D}_{\mathrm{photon}}$, when the photon plans are scaled such that they lead to the same NTCP as their proton counterpart. We use Equation 10 to search for a scale factor f, such that the scaled photon dose distribution $f\boldsymbol{D}_{\mathrm{photon}}$ in N fractions gives the same gEUBED_n as protons. The dose escalation potential of protons is $\frac{D^{\mathrm{GTV}}_{\mathrm{proton}}}{fD^{\mathrm{GTV}}_{\mathrm{photon}}}$, which is the ratio

of the average GTV doses in the (delivered) proton dose distribution and the scaled (planned) photon dose distribution. The ratio will clearly depend on the chosen volume parameter n and the fractionation sensitivity α/β, however, not on the fraction size fs used to adjust for fractionation (see Section A). For $\alpha/\beta = \infty$ the ratio signals the dose escalation potential based purely on physical dose, whereas for $\alpha/\beta < \infty$ the dose escalation also takes into account the effects of fractionation. In order to estimate the dose escalation potential for standard fractionation as well, we perform the same calculations by considering scaled proton plans delivering 70 Gy to the GTV in $N = 35$ fractions as the reference. Therefore, we also determine the scale factors f such that the scaled photon dose distributions $f\boldsymbol{D}_{\text{photon}}$ in $N = 35$ fractions give the same gEUBED_n values as the scaled proton dose distributions $70\,\text{Gy}/D^{\text{GTV}}_{\text{proton}} \cdot \boldsymbol{D}_{\text{proton}}$ in $N = 35$ fractions, yielding the dose escalation potential of protons for standard fractionation as $\dfrac{70\,\text{Gy}}{fD^{\text{GTV}}_{\text{photon}}}$.

Throughout the paper relative biological effectiveness (RBE) is taken into account by adjusting proton doses with $\text{RBE}_{\text{proton}} = 1.1$. BED calculations are done subsequent to the RBE adjustment using Equation 1 and all presented proton dose values are the RBE corrected doses $D_{\text{proton}} = \text{RBE}_{\text{proton}} \cdot \tilde{D}_{\text{proton}}$. In [34] Dale and Jones introduced a modified BED formulation that allows the direct incorporation of RBE effects. Our theoretical models can be generalized accordingly, and the differences between the two approaches are relatively small (for a detailed discussion and a comparison of the results see Section C).

2.5 Patient Data

We analyzed 24 liver cancer patients with varying tumor size, location and recurrence status. Patients underwent a 2 day CT simulation to assess internal motion and reproducibility. Plans were created using mid-ventilation CT (30% phase) where the tumor volume was derived from arterial/venous phase contrast CT scan fused to the planning CT.

All patients were treated with passively scattered protons in 5 or 15 fractions, with prescription doses of 40 Gy or 50 Gy for the former; and between 45 Gy to 67.5 Gy for the latter schedule. Proton plans incorporated aperture expansion and compensator smearing based on measured internal organ motion, utilizing 2-3 fields per plan. For research purposes, IMRT plans were also made for the patients, using the same target volumes, 7-10 treatment fields, and standard clinical planning procedures. Since the passively scattered protons were used for treatment and liver motion was considerable, proton plans typically employed larger margins than their photon counterparts to avoid potential loss of target coverage. For all proton and photon plans the mean dose and the dose variance were calculated for the healthy liver (liver minus the Clinical Target Volume), and subsequently the dose shape factors were determined. For analysing the dose variance in Section 3.1 and the example patient in Section 3.3.1, the IMRT plans were scaled such that the healthy liver mean physical dose matched that of their proton counterpart. For the calculations of case 4 (Section 3.5) IMRT plans were scaled according to Equation 10, such that the healthy liver gEUBEDs were identical to those of the proton plans for a range of volume parameters $n \in [0, 1.2]$ and three different fractionation sensitivity values of $\alpha/\beta \in \{2, 4, \infty\}$ Gy.

3 Results

3.1 Dose Variance and Dose Shape Factor of Proton and Photon Plans

Figure 1 gives an overview of the dose differences between proton and photon plans. There is a clear distinction in terms of the dose variance (Figure 1a): proton plans have higher dose variance for the same mean healthy liver dose. The distinction in terms of dose shape factor φ becomes apparent in Figure 1b showing the dose shape factor as a function of the relative liver dose (i.e. the fraction of the mean dose in the healthy liver and the GTV). Photon plans have smaller dose shape factors than proton plans. The average dose shape factor across all photon plans is 2.2, whereas the average dose shape factor for proton plans is 4.0. Furthermore, as shown in Figure 1b, there is a decreasing trend of φ with the relative mean dose (for the fit results see Section 2 of the Supplementary Materials (SM)). This is intuitive: lower relative mean dose signals better dose sparing, which inevitably leads to more dose variation in the organ.

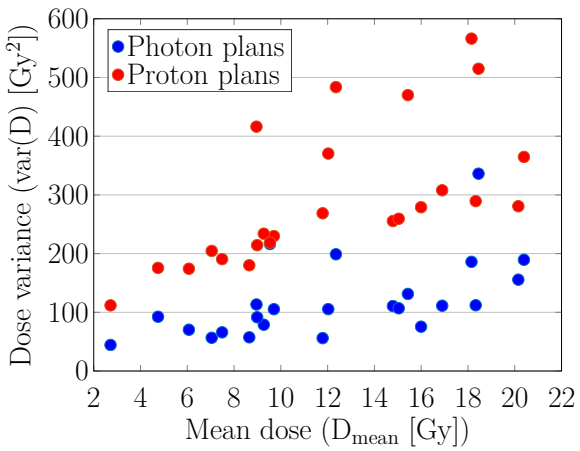

(a) Distribution of the healthy liver mean dose and dose variance values. Photon dose distributions scaled to the same mean dose as their proton counterparts.

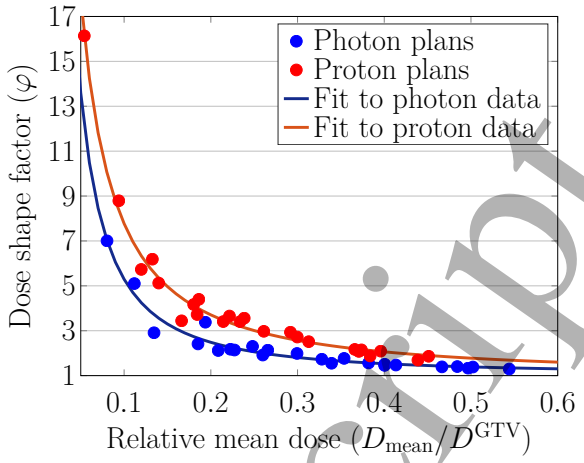

(b) Dose shape factors φ for photon and proton plans as a function of the relative healthy liver mean dose.

Figure 1. Comparison of the photon and proton dose distributions in the healthy liver (liver minus CTV).

3.2 Calculating Iso-Effective Mean Doses in New Fractionation Schemes (Case 1)

3.2.1 Analysis of Proton and Photon Plans

Figure 2 demonstrates the effects of the dose shape factor when iso-effective mean doses in new fractionation schemes are calculated for commonly used liver mean dose tolerances [5, 23, 31] and $\alpha/\beta^{Liver} = 4\,\text{Gy}$. First, we calculate the dose to be delivered in 5 fractions that is equivalent with 30 Gy in 35 fractions, a widely applied mean dose constraint in standard fractionation (blue lines, Figure 2a). The traditional BED formulation (Equation 3) yields an equivalent 5-fraction dose of 18.8 Gy (dashed line). In contrast, when the calculation is done employing Equation 7 (using $\varphi_{ref} = \varphi_{new} \geq 1$), the 5-fraction doses are systematically lower (solid line). E.g. for a commonplace value of $\varphi = 3$ the equivalent dose is 15 Gy, 20% lower than 18.8 Gy. Second, we calculate the dose in 35 fractions that is equivalent to 17 Gy in 5 fractions (red lines). The standard BED formulation yields 26.5 Gy, whereas the mean BED equivalent doses are up to 40% higher for realistic φ values.

Figure 2b quantifies this effect for clinical treatment plans. The healthy liver mean doses D_{ref} in the proton plans - delivered in 5 or 15 fractions - were converted to equivalent 35-fraction doses D_{new} ($N_{\text{ref}} = 5$ or 15, $N_{\text{new}} = 35$, $\varphi_{\text{ref}} = \varphi_{\text{new}}$ corresponding to the proton dose shape factors), in order to compare them to proton treatments with standard fractionation. The truly mean BED equivalent 35-fraction doses are systematically and significantly higher than what the traditional BED formulation (Equation 3) suggests. Differences up to 8 Gy (+40%) can be observed. Moreover, while all plans seem safe according to the simple BED model having 35-fraction mean doses below 30 Gy, for 1 patient the mean BED equivalent mean dose is 5 Gy higher than the tolerance.

3.2.2 Analysis of the Protocol of a Phase II Randomized Trial for Hepatocellular Carcinoma

In the NRG-GI003 cooperative group clinical trial protocol [26] (clinicaltrials.gov identifier NCT03186898, currently recruiting patients) liver tolerances are given as prescription dose dependent values, separately for 5- and 15-fraction treatments (shown in black in Table I). Assuming $\alpha/\beta^{Tumor} = 10\,\text{Gy}$, the prescription dose levels in the 2 fractionation schemes (columns 1 and 2) are approximately iso-effective: e.g. 50 Gy in 5 fractions and 67.5 Gy in 15 fractions both represent $\approx 100\,\text{Gy}_{10}$ BED. The corresponding tumor BED values (shown in blue, column 3) are monotonically decreasing with decreasing prescription dose.

Columns 4 and 5 show the mean dose constraints for the healthy liver for 5 and 15 fractions, respectively. Making the 4 dose tolerance pairs belonging to the same tumor BED levels BED equiva-

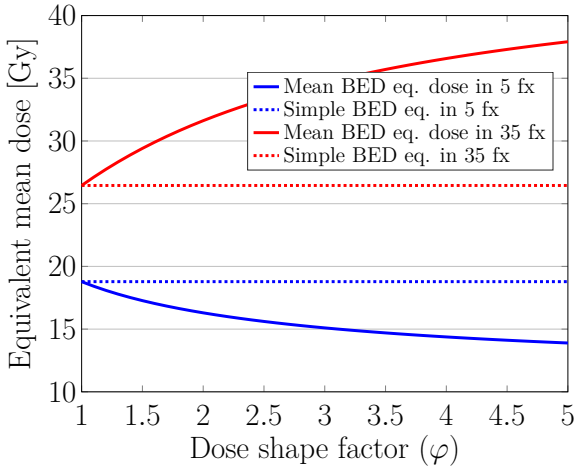

(a) Mean doses in 5 and 35 fractions that are BED equivalent to 30 Gy in 35 fractions and 17 Gy in 5 fractions respectively.

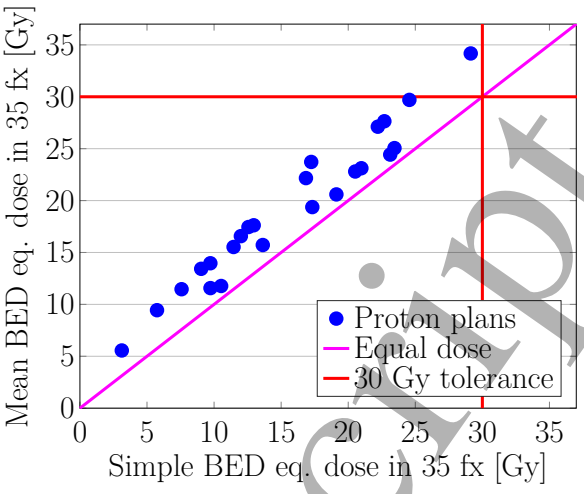

(b) Mean doses in 35 fractions that are equivalent with the given proton doses in 5/15 fractions, with (y-axis) and without (x-axis) taking into account the dose shape.

Figure 2. Difference between taking into account vs. neglecting the effects of the dose distribution when calculating iso-effective mean doses between fractionation schemes. Panel (a) presents a theoretical case showing the mean doses that are BED equivalent to 2 clinically used liver mean dose constraints as a function of the dose shape factor. Panel (b) highlights the BED equivalent liver mean doses using the data from our patient cohort.

lent requires unrealistically low $\alpha/\beta_{eq} \in [0.17, 1.14]$ Gy values (shown in red in Table I) if the simple BED formula (Equation 2) is used. Furthermore, the resulting equivalent liver BED levels BED_{eq} vary non-monotonically. Using a realistic $\alpha/\beta^{Liver} = 4$ Gy value in Equation 3 to calculate the 15-fraction equivalent of 5-fraction tolerances yields doses (shown in yellow) 4 Gy to 6 Gy (more than 20%) below the actual values. Consequently, the used liver tolerance values are not consistent with the traditional BED formalism.

Table I. Mean liver tolerances for 5 and 15 fractions in the NRG-GI003 cooperative group clinical trial protocol. Calculated tumor BEDs are shown in blue (column 3). The α/β_{eq} values making the liver dose constraints (columns 4 and 5) corresponding to the same tumor BED level equivalent and the equivalent liver BED_{eq} values are displayed in red (columns 6 and 7). 15-fraction liver mean dose tolerances calculated from the 5-fraction values using $\alpha/\beta = 4$ Gy and the traditional BED formulation are in yellow (column 8), whereas the values calculated by taking into account the dose shape differences are in cyan (last column).

Prescription dose[a]		Tumor BED[b]	Used constraints[a]		α/β_{eq}[c]	BED_{eq}[d]	Calculated 15 fx constraints[a]	
$N = 5$	$N = 15$		$N = 5$	$N = 15$			W/o shape	With shape
50	67.5	100/97.88	13	22	0.17	211.4	16.77	20.91
45	58.05	85.5/80.52	15	24	0.74	76.36	19.75	24.70
40	N/A	72/N/A	15	N/A	N/A	N/A	19.75	24.70
35	45	59.5/58.5	15.5	24	1.14	57.82	20.51	25.65
30	37.5	48/46.88	16	27	0.24	232.6	21.26	26.61
27.5	N/A	42.63/N/A	17	N/A	N/A	N/A	22.79	28.53

[a] Physical dose values are in units of Gy.
, [b] BED values are calculated using $\alpha/\beta^T = 10$ Gy, and are displayed as 5 fraction BED/15 fraction BEDs in Gy_{10} units.
, [c] α/β values displayed in units of Gy.
, [d] Equivalent BED values displayed in units of α/β_{eq}, i.e. the α/β that makes the liver mean dose constraints BED equivalent using the simple BED formula (Equation 2).

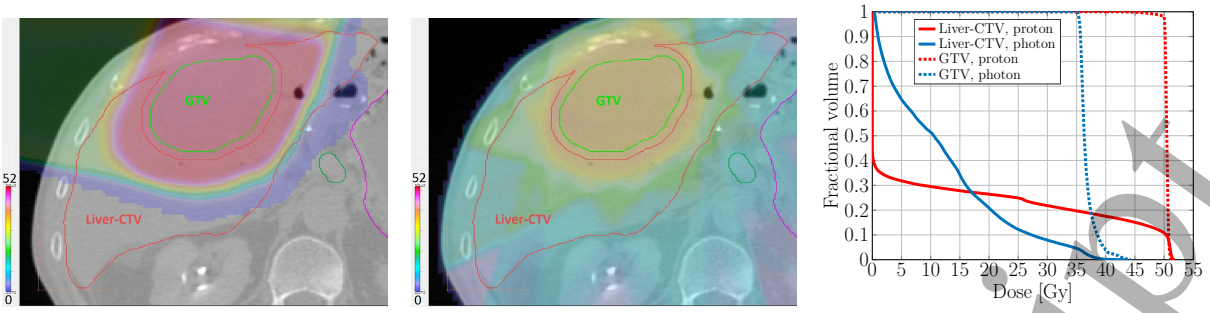

(a) Dose distribution in the proton plan.

(b) Dose distribution in the photon plan (dose scaled to the same mean liver dose as in the proton plan).

(c) The DVHs of the healthy liver and the GTV in the proton and the scaled photon plans.

Figure 3. Difference between proton and photon dose distribution for a liver patient. The photon distribution was scaled to the same mean liver dose as in the proton plan, thus has significantly lower GTV dose.

The average dose shape factor of the photon plans for the patients treated with 15 and 5 fractions is $\varphi^{15}_{\text{photon}} = 1.80$ and $\varphi^{5}_{\text{photon}} = 2.49$, respectively. Using these values in Equation 7 to extrapolate the 5-fraction doses to 15 fractions (i.e. $\varphi_{\text{ref}} = \varphi^{5}_{\text{photon}}$, $\varphi_{\text{new}} = \varphi^{15}_{\text{photon}}$, $N_{\text{ref}} = 5$ and $N_{\text{new}} = 15$) results in the doses shown in cyan in Table I, corresponding far better to the actual mean dose tolerances (within 0.3 Gy to 1.6 Gy).

3.3 Calculating Iso-Effective Mean Doses in New Modalities (Case 2)

3.3.1 Detailed Analysis of a Selected Patient

We present a detailed analysis of a patient where the difference between the proton and photon plans was significant. The patient received proton treatment delivering $D^{\text{GTV}}_{\text{new}} = 50.4\,\text{Gy}$ in 5 fractions to the target volume, and $D_{\text{new}} = 12\,\text{Gy}$ mean dose to the healthy liver. The corresponding dose distribution is plotted in Figure 3a, the DVHs in Figure 3c. 60% of the liver was completely spared, whereas the part close to the target received the full prescription dose. The relative liver dose is therefore low, $D_{\text{new}}/D^{\text{GTV}}_{\text{new}} = 0.239$, while the dose variance is high, $var\,(\boldsymbol{D}_{\text{new}}) = 370\,\text{Gy}^2$. Consequently the dose shape factor is relatively large, $\varphi_{\text{new}} = 3.561$.

The dose distribution in the (9 field) photon plan - that is scaled to the same mean liver dose as the proton plan - is shown in Figure 3b, with the corresponding DVHs in Figure 3c. No part of the healthy liver is completely spared, hence the relative dose is higher than in the proton plan, $D_{\text{ref}}/D^{\text{GTV}}_{\text{ref}} = 0.328$, but the dose variance is smaller, $var\,(\boldsymbol{D}_{\text{ref}}) = 105.4\,\text{Gy}^2$. Consequently, the dose shape factor is smaller, $\varphi_{\text{ref}} = 1.730$ (for details on why proton plans generally have higher φ, see Section 1.2 of the SM).

Due to the shape difference, the same 12 Gy mean liver dose leads to significantly different mean BEDs of $37.64\,\text{Gy}_4$ for protons and $24.46\,\text{Gy}_4$ for photons ($\alpha/\beta^{Liver} = 4\,\text{Gy}$). Equation 6 reveals that the proton plan is mean BED equivalent to a photon plan with a mean dose of 15.87 Gy, more than 30% higher than 12 Gy. Conversely, if the proton plan was scaled to have identical mean BED to its photon counterpart, the proton mean dose would be 9.24 Gy, 23% lower than 12 Gy. Hence, while protons allow a dose escalation of 35% (i.e. a target mean dose of 50.4 Gy vs. 36.9 Gy with photons, see Figure 3c) by matching the liver mean physical dose levels in the 2 modalities, this reduces to only 5% (proton target dose of 38.6 Gy) when matching the mean BEDs.

3.3.2 Quantifying the Effects of Shape Difference

Figure 4 highlights the effects of the dose shape factor when iso-effective mean doses are calculated in different modalities. Figure 4a shows the additional dose $\Delta D = D_{\text{ref}} - D_{\text{new}}$ in a reference modality (with $\varphi_{\text{ref}} = 2$, typical for IMRT) as a function of the shape difference $\Delta\varphi = \varphi_{\text{new}} - \varphi_{\text{ref}}$ between two modalities for $N_{\text{ref}} = N_{\text{new}} = 5$ and different D_{new} values. The additional dose increases both with the difference in the spatial distribution $\Delta\varphi$ and with the mean dose D_{new} in the new modality, whereas

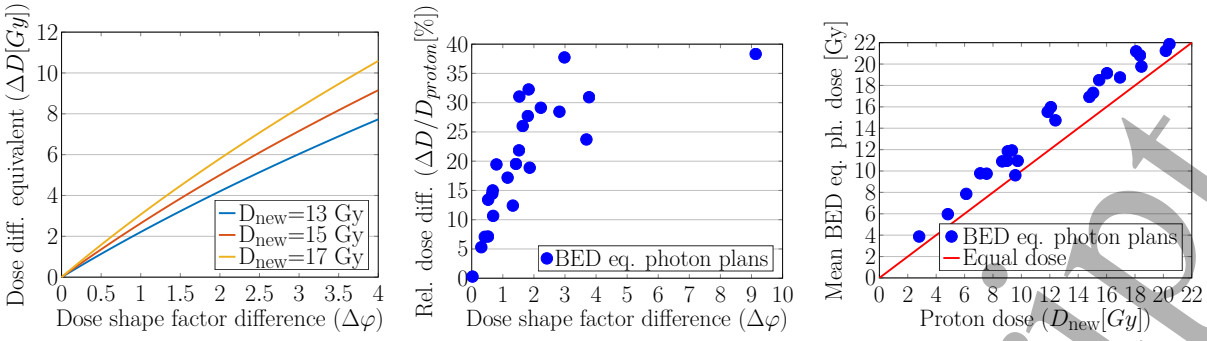

(a) Additional dose in a 5-fraction plan with a dose shape factor of $\varphi_{ref} = 2$ due to higher dose inhomogeneity ($\Delta\varphi$).

(b) Relative dose difference resulting from the dose shape difference between proton and photon plans.

(c) Mean BED equivalent photon mean dose as a function of proton mean dose.

Figure 4. Dose effects of shape differences.

it decreases with the reference dose shape factor φ_{ref}. The dose difference can get substantial for large shape differences: e.g. for a shape difference of $\Delta\varphi = 3$, a 5-fraction mean dose of 17 Gy in the new modality is equivalent to a mean dose of 25 Gy in the reference modality, representing a +50% increase.

To quantify effects for clinical treatment plans, proton mean liver doses D_{new} (with dose shape factor φ_{new}) were converted to mean BED equivalent photon mean doses $D_{\text{ref}} = D_{\text{new}} + \Delta D$ (with dose shape factor φ_{ref}) for all 24 patients, using the clinically delivered number of fractions for $N_{\text{new}} = N_{\text{ref}}$. Figure 4b displays the resulting additional mean dose ΔD relative to the proton dose as a function of the shape difference $\Delta\varphi = \varphi_{\text{new}} - \varphi_{\text{ref}}$. Generally, higher dose shape differences lead to higher relative dose differences, reaching 30-40% (in agreement with the theoretical results shown in Figure 4a). In absolute terms, the mean BED equivalent photon doses are 1 Gy-4 Gy higher than the proton doses (Figure 4c).

3.4 Potential Dangers of Neglecting the Shape Effect (Case 3)

To study whether the additional dose due to shape differences can be potentially unsafe, Figure 5 displays the mean BED equivalent 35-fraction photon mean doses (i.e. the results of Equation 6) vs. the simple BED equivalent mean doses (i.e. the results of Equation 3). When the traditional BED formula is used (Equation 2), all 35-fraction doses are below the 30 Gy liver tolerance [5, 31]. When the proton-photon shape differences are accounted for (Equation 6) the mean dose is above 30 Gy in two cases (for a discussion of the 30 Gy tolerance see Section 3 of the SM.).

3.5 Dose Escalation Potential of Proton Therapy (Case 4)

The ratio of the proton/scaled photon GTV doses - having identical gEUBED values for the healthy liver according to Equation 10 - averaged over the 24 patients can be seen in Figure 6 for three different α/β ratios and a range of volume parameters $n \in [0, 1.2]$. There are three findings:

- When $0 < n < 0.6$, photon plans are generally better based on the physical dose, which is a result of penalizing the larger high dose region of proton plans in the gEUD calculations. The only exception is $n = 0$ (when only the maximum point dose in the healthy liver matters), primarily caused by the slightly better homogeneity of proton plans in the GTV (see Figure 3c), typically leading to higher average GTV doses for the same maximum point dose.
- For $n > 0.6$, protons are clearly better in terms of physical dose, as the low dose bath of photon treatments starts to limit the GTV dose for a given gEUD value. For $n = 1$ on average a 25% dose escalation potential can be observed for the same liver mean physical dose, well corresponding to the 35% dose escalation found for the patient in Section 3.3.1 (case 2).
- Most importantly, adjusting for fractionation ($\alpha/\beta < \infty$) significantly influences the achievable benefit of protons. Except for small volume parameters ($n \approx 0$), photons remain generally better

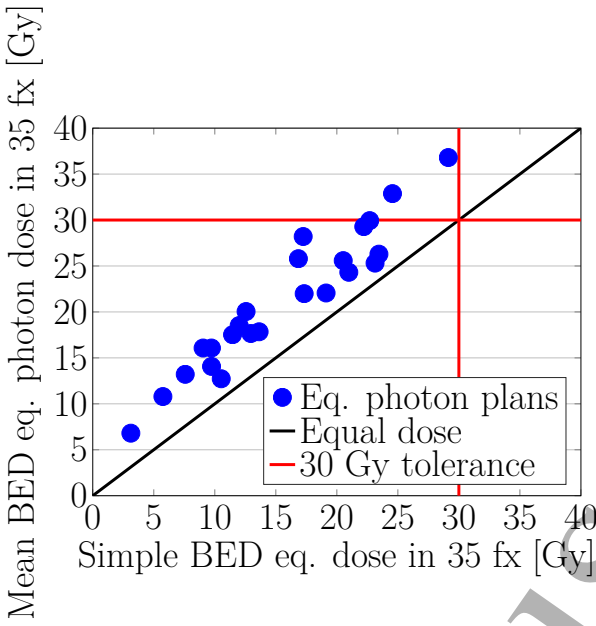

Figure 5. Mean BED equivalent 35-fraction photon mean doses versus simple BED equivalent 35-fraction mean doses.

till around $n \approx 0.6$ (also see Figure 8 in Section C). For higher volume parameters ($n > 0.6$) proton plans become better, but the BED adjustment increasingly penalizes them - mainly due to their high dose region - decreasing their benefits. For the hypofractionated, clinical proton plans (Figure 6a) we only see a 5% average dose escalation potential for $n = 1$ with $\alpha/\beta = 4\,\text{Gy}$ (vs. 25% based on physical dose), increasing to 10% (vs. 35%) for $n = 1.1$ (the value previously found for liver in [35]). For standard fractionation (Figure 6b) the degradation is less substantial, but is still significant, only allowing for 15%/20% higher target doses with protons for $n = 1/1.1$ (instead of 25%/35%). For a more detailed discussion of how the method of incorporating RBE affects the dose escalation potential, see Section C.

4 Discussion

Regarding the Dose Shape Effects The dose shape factor has an opposite effect when deriving doses for less and more fractions (Figure 2a). The truly mean BED equivalent doses are always lower than what the traditional BED formalism (Equation 2) suggests when deriving doses for more hypofractionated schedules. Hence the standard BED equation leads to potentially unsafe, higher dose tolerances than intended. Conversely, neglecting the dose shape factor when calculating the equivalent of hypofractionated mean doses in traditional fractionation schemes results in lower values than what is mean BED equivalent. Therefore the simple BED formalism underestimates the effects of mean doses in hypofractionated schedules (Section 1.3 of the SM provides a mathematical proof of this duality).

Mean doses in plans with high dose variance could be mean BED equivalent to vastly (50%) higher mean doses in less inhomogeneous plans (Figure 4a). Clinical treatment plans indeed exhibit such sizable dose differences (Figures 4b-4c). Therefore, applying mean dose tolerances established for one modality on-to-one to another with significantly more inhomogeneous dose distribution should be done with caution, as this may lead to dose constraints that are too high. Instead, it is better to establish dose tolerances according to Equation 7 by taking into account the (typical) differences between the dose distributions of the two modalities.

The shape effect is especially important when the organ in question is the dose limiting structure, so that its mean dose is close to its tolerance. For example, this is the case for liver tumors treated in a dose escalation protocol where the liver mean dose meets the constraint in order to maximize the

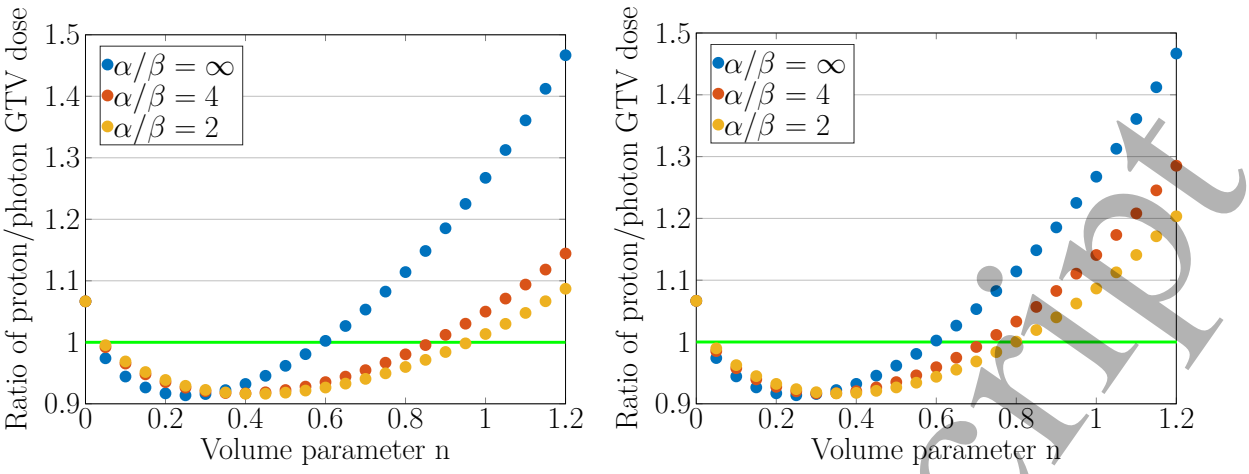

(a) Reference: hypofractionated (5/15 fraction), clinically delivered proton plans.

(b) Reference: scaled proton plans assuming standard fractionation (70 Gy GTV dose with 2 Gy/fx, 35 fractions).

Figure 6. Dose escalation potential of protons vs. photons for equivalent gEUD based NTCP values with various volume parameters n and fractionation sensitivities α/β.

prescription dose [26]. If a mean dose constraint was derived from patients treated with photon beams, and the patient is treated with proton beams to the maximally allowed mean dose, the proton treatment will typically violate the constraint in terms of mean BED. In our patient cohort on average protons allowed for 25% dose escalation compared to photons for the same physical liver mean dose (as shown in Figure 6). When dose escalation is instead performed based on mean liver BED, protons allowed for only marginally ($\approx 5\%$) higher prescription doses. Although this degradation of proton dose escalation potential is less severe if standard fractionation is assumed for the plans ($N = 35$ fractions, 70 Gy proton target dose with 2 Gy/fx), it was still significant, only allowing for $\approx 15\%$ higher proton doses.

Regarding Mean BED Tolerances Our results are not specific for mean doses. As Figure 6 (and Figure 8) highlight the dose escalation potential of proton therapy is significantly decreased for a wide range of volume parameters ($n > 0.6$) when using a gEUD based NTCP model taking into account fractionation. Hence while there is considerable uncertainty regarding the dose-volume effects in the liver (and in other OARs in general), regardless of what the exact value of volume parameter is, the dose shape, and specifically the larger margins of proton dose distributions compared to photon dose distributions have an important effect on tolerances. These larger high dose areas get emphasized when adjusting for fractionation, and consequently result in higher NTCP values in general. Therefore, within the validity of gEUD based NTCP models including fractionation effects, proton plans are indicated to result in higher normal tissue complications than what could be expected purely from the physical dose distribution.

As a result, the dose escalation potential of protons is substantially reduced if mean BED (or in general gEUBED) rather than mean physical dose (or gEUD) is the relevant metric to limit toxicity. Based on the outcome data from photon treatments, this may indeed be the case e.g. for the liver and the lung [31, 36]. These works conclude that the volume parameter is close to $n = 1$ in these organs and the mean of the fraction-size adjusted dose distribution - which is only different from the mean BED up to patient-independent constant factor, see Equation 11 in Section A - correlates with organ damage. In fact, the liver SBRT protocol of [37] already describes the clinical use of such a mean BED constraint, since the authors employ an LKB model based dose escalation scheme with a volume parameter of $n = 0.97$ to determine individualized prescription doses for given NTCP values (5%, 10% or 20%).

In general, hepatotoxicity data from the published literature is always difficult to compare, mainly due to considerable variation across studies in patient population, treatment regimens, exact definition of radiation induced liver disease (RILD), etc. Moreover, research specifically focusing on analysing the outcomes from proton vs. photon radiation therapy for RILD is rare [38]. Thus, in the context of

comparing protons and photons for liver SBRT in particular, it is not clear whether mean physical dose, mean BED, or some other metric is the most relevant for tissue damage. Preliminary data from our own institution suggests that liver function is better preserved in proton therapy than in photon therapy. A mean dose/BED constraint may therefore underestimate proton's advantage of avoiding the low dose bath in a significant portion of the liver. If instead a DVH point for the low dose bath is the relevant metric for example, the dose escalation potential of protons is substantially higher. A commonly used constraint for the liver in SBRT protocols, the sparing of at least 700 cm^3 of the healthy liver to less than 15 Gy in 3-6 fractions [23, 39] indeed suggests that this may be the case. Based on this metric, should a proton plan deliver virtually no dose to at least 700 cm^3 of the liver, its dose escalation potential would be infinite.

Regarding Relative Biological Effectiveness and Margins Throughout the paper RBE effects were taken into account by adjusting proton doses with $\mathrm{RBE}_{\mathrm{proton}} = 1.1$. Therefore all presented and plotted proton doses were the RBE adjusted doses $D_{\mathrm{proton}} = \mathrm{RBE}_{\mathrm{proton}} \tilde{D}_{\mathrm{proton}}$ and all BED calculations were done subsequent to the RBE adjustment. This can be considered a simplified approach, but is consistent with current clinical practice, where the proton RBE is assumed to be fraction-size independent. Dale and Jones [34] introduced a modified BED formulation that allows for the incorporation of RBE effects. The differences between the two formulations are discussed in details in Section C. The main conclusion is that the presented theory can easily be generalized according to [34], and for protons - having an RBE relatively close to unity - the exact method of accounting for RBE is only of minor importance, with the Dale-Jones RBE methodology predicting 5-10% smaller effects than our constant RBE model.

A central focus of the paper is to study the effects of the dose shape. Clearly, the shape of the dose distribution is closely connected to the employed margins in the proton (and photon) plans. Margins in turn strongly depend on the considered organ motion, motion mitigation techniques as well as the choice of proton delivery method (passive scattering or pencil beam scanning). Since our patient cohort focused on liver cases (having relatively large motion uncertainties) treated with passively scattered protons, and these proton plans were compared to state-of-the-art IMRT, our results likely represent a worst case scenario for protons. For treatment sites with less motion, where better immobilization and motion mitigation methods can be applied (e.g. brain), effects will be smaller. Additionally, advances in on-line proton range verification methods are expected to decrease proton planning margins, which will further reduce the current disadvantage of protons, i.e. the irradiation of larger areas around target structures with the prescription dose compared to photons.

Regarding the Context of Our Work The main novelty of our work is a practical, but consistent methodology that allows the establishment of (primarily) mean dose tolerances in new fractionation schemes and new treatment modalities, such that they are iso-toxic as assessed from NTCP models. Essentially, we achieve this by building on established radiobiological models (BED, DVHs and gEUD) to arrive to the formulation of the gEUBED. These concepts are all well known and have been validated in clinical practice. However, they mainly represent phenomenological descriptions reflecting the experience with fractionation (for BED) and volume effects (for DVH and gEUD), rather than a detailed understanding of the exact radiobiological mechanisms underlying organ damage. As any model, they unavoidably have their limitations. For example, the accuracy of the BED model to high dose per fraction values has been debated excessively for decades, without final resolution [40, 41]. Summarizing three-dimensional dose distributions by DVHs disregards where the dose is deposited exactly, therefore cannot account for varying radiation sensitivity within the organ or the relative importance of some functional sub-units over others for overall organ function. gEUD is a completely empirical concept: the volume parameter is derived purely from experience and there is no known radiobiological justification behind its mathematical form. Since our work builds on these concepts instead of using first principles, it necessarily inherits all their shortcomings as well. Simply put, our message is that - regardless of the actual underlying radiobiology - the presented approach is useful for its the intended purpose: to establish mean dose tolerances in a more meaningful way than currently possible, taking into account fractionation, dose shape and possibly RBE (see Section C) effects.

Despite these limitations of our study (and the fact that it is an in-silico comparison for patients for whom outcome data is not yet available), it well justifies a warning and discussion regarding the

use of mean dose - and in general gEUD - constraints for proton therapy that were derived for photon therapy. As first reported by [42], photon-derived normal tissue complication models may indeed be relatively well applicable to proton therapy treatments as well. Though the derivation of proton specific NTCP models is naturally expected to remain an active research area, until such models are obtained and validated, only the currently available ones can be used (e.g. to guide patient selection eligible for proton treatments [43]). These (fraction-size adjusted) gEUD based NTCP models indicate that proton therapy's dose escalation potential may be reduced for a wide range of volume parameters, especially for treatment sites with significant organ motion requiring large margins, warranting caution when using a physical dose based escalation strategy. Similar care should be taken when applying photon therapy based physical dose constraints to proton treatments, as they may overestimate tolerable doses due to the significantly different dose distributions.

5 Conclusions

When mean dose tolerances are chosen for new fractionation schemes or irradiation modalities the shape of the dose distribution should be accounted for. The traditional BED formalism tends to overestimate tolerances when they are calculated for more hypofractionated regimes. In addition, mean tolerance values - and gEUD tolerances in general - established for one modality cannot necessarily be applied to other modalities having drastically different dose distributions. The formalism introduced in this paper allows the incorporation of the spatial dose distribution into BED based estimation of mean dose constraints, which can help alleviating these issues.

A Compatibility of Mean BED Equivalent and Iso-NTCP Based Derivation of Mean Dose Constraints

Let us suppose we have an organ that receives a dose distribution $\boldsymbol{D} = (D_1, ..., D_M)$ in N fractions (M is the number of voxels). To calculate the associated NTCP value, most models rely on using the generalized Equivalent Uniform Dose (the popular Lyman-Kutcher-Burman (LKB) approach also belongs to this category, see Section B). When using any gEUD based NTCP model with a fractionation component (as in [44, 36, 45, 46, 47, 31]) the following three steps are made [48, 18]:

- First, the doses are adjusted for fraction size, i.e. a dose distribution is calculated which - if given in uniform fractional doses fs in each voxel - is BED equivalent to the original dose. This dose in voxel i is

$$D_{adj,i} = D_i \frac{1 + \frac{D_i}{N\alpha/\beta}}{1 + \frac{fs}{\alpha/\beta}} = \frac{\mathrm{BED}_i}{1 + \frac{fs}{\alpha/\beta}}. \tag{11}$$

  [49] appropriately calls Equation 11 the "Fraction-size Equivalent Dose" and [50] refers to it as "Equieffective Dose". If the fraction size is $fs = 2\,\mathrm{Gy/fraction}$ Equation 11 is the well-known Normalized Total Dose (NTD) [21, 51, 52] or Equivalent Dose delivered in 2 Gy fractions (EQD2).

- Next, using the fraction size adjusted dose distribution, the generalized Equivalent Uniform Dose is calculated for a chosen volume parameter n [2] as

$$\mathrm{gEUD}_n\left(\boldsymbol{D}_{adj}\right) = \left(\frac{1}{M}\sum_{i=1}^{M} D_{adj,i}^{1/n}\right)^n = \left(\frac{1}{M}\sum_{i=1}^{M}\left(\frac{\mathrm{BED}_i}{1 + \frac{fs}{\alpha/\beta}}\right)^{1/n}\right)^n =$$

$$\frac{\left(\frac{1}{M}\sum_{i=1}^{M}\left(\mathrm{BED}_i\right)^{1/n}\right)^n}{1 + \frac{fs}{\alpha/\beta}} = \frac{\mathrm{gEUD}_n\left(\mathbf{BED}\left(\boldsymbol{D}, N, \alpha/\beta\right)\right)}{1 + \frac{fs}{\alpha/\beta}} = \frac{\mathrm{gEUBED}_n\left(\boldsymbol{D}, N, \alpha/\beta\right)}{1 + \frac{fs}{\alpha/\beta}}. \tag{12}$$

We used the notation $\mathrm{gEUBED}_n\left(\boldsymbol{D}, N, \alpha/\beta\right)$ to signal a $\mathrm{gEUD}_n\left(\mathbf{BED}\left(\boldsymbol{D}, N, \alpha/\beta\right)\right)$ calculation based on the BED distribution $\mathbf{BED}\left(\boldsymbol{D}, N, \alpha/\beta\right) = \left(\mathrm{BED}_1, \mathrm{BED}_2, ..., \mathrm{BED}_M\right)$, corresponding to giving a dose distribution $\boldsymbol{D}$ in N fractions to an organ with fractionation sensitivity α/β (as opposed to a $\mathrm{gEUD}_n\left(\boldsymbol{D}\right)$ calculation based on the physical dose distribution $\boldsymbol{D}$ directly). Simply stated, Equation 12 means that if we adjust for fractionation, the gEUD in an organ is a constant factor times the "generalized Equivalent Uniform BED" [33]. This constant factor is $1/\left(1 + fs/\alpha/\beta\right)$, only depending on the chosen fraction size fs and the α/β ratio. In the literature Equation 12 has also been called the "modified Equivalent Uniform Dose" [53] and the "radiobiologically corrected gEUD" [18].

- Last, normal tissue complication probability is calculated as

$$NTCP = h(\mathrm{gEUD}_n\left(\boldsymbol{D}_{adj}\right)) = \frac{1}{1 + \left(\frac{TD_{50}}{\mathrm{gEUD}_n\left(\boldsymbol{D}_{adj}\right)}\right)^{\gamma_{50}}} \tag{13}$$

where the given logistic function in Equation 13 is only one possibility, in general there are several possible forms for $h\left(\mathrm{gEUD}_n\left(\boldsymbol{D}_{adj}\right)\right)$.

Under this approximation two dose distributions $\boldsymbol{D}_{\mathrm{ref}}$ in N_{ref} fractions and $\boldsymbol{D}_{\mathrm{new}}$ in N_{new} fractions will be iso-effective if they lead to the same NTCP given by Equation 13. However, for a chosen NTCP model (e.g. for fixed TD_{50} and γ_{50} parameters in a logistic model) this equivalence simply requires that after adjusting for fractionation the two dose distributions give identical gEUDs according to Equation 12. Consequently, if the same fraction size fs is used to adjust doses for fraction size, the equivalence further simplifies to the equivalence of the "generalized Equivalent Uniform BEDs", i.e. to

$$\mathrm{gEUBED}_n\left(\boldsymbol{D}_{\mathrm{ref}}, N_{\mathrm{ref}}, \alpha/\beta\right) = \mathrm{gEUBED}_n\left(\boldsymbol{D}_{\mathrm{new}}, N_{\mathrm{new}}, \alpha/\beta\right),$$

which for a parallel structure ($n = 1$) leads to Equation 6. Hence our mean BED equivalent derivation for a mean dose tolerance D_{mean} in a new fractionation scheme with N_{new} number of fractions is simply a special case of requiring the generalized EUD based NTCP values of the new and the reference dose distributions to be identical for a parallel structure.

B The Dependence of the Lyman-Kutcher-Burman (LKB) NTCP Model on the gEUD

In [54] it is proven that "the EUD for an OAR calculated by the generalized Niemierko formula yields a dose which, if applied uniformly to the entire volume of the OAR, would result in the same NCTP as the effective volume Kytcher-Burman DVH reduction algorithm, calculated for any reference dose." Essentially the authors of [54] have already shown that the classic LKB model of NTCP can be reformulated to depend on the gEUD_n, furthermore [55] also highlights it, but for clarity this is explicitly pointed out here.

In the Lyman model [56] the NTCP for a uniform irradiation of a fraction $v = V/V_{ref}$ of an organ to dose D depends on a parameter

$$u = \frac{D - TD_{50}(v)}{m \cdot TD_{50}(v)},$$

where $TD_{50}(v) = TD_{50}(1) \cdot v^{-n}$ and $TD_{50}(1)$ are the partial-volume-dependent and whole organ doses for 50% complication probability and m characterizes the steepness of the dose response. For inhomogeneous organ irradiation the Kutcher-Burman volume reduction is used [29], resulting in the effective volume

$$v_{eff} = \sum_{j=1}^{M} v_j \left(\frac{D_j}{D_{ref}}\right)^{\frac{1}{n}},$$

where v_j is the relative volume of element j ($\sum_{j=1}^{M} v_j = 1$) receiving a normalized dose D_j/D_{ref} for a reference dose D_{ref}. The assumption is that irradiation a v_{eff} fractional volume of the organ with dose

D_{ref} would result in the same complication probability as the inhomogeneous irradiation. Correspondingly, the final NTCP value in the LKB model depends on

$$u = \frac{D_{ref} - TD_{50}(v_{eff})}{m \cdot TD_{50}(v_{eff})}.$$

However, this dependence can be reformulated as

$$u = \frac{D_{ref} - \frac{TD_{50}(1)}{v_{eff}^n}}{m \cdot \frac{TD_{50}(1)}{v_{eff}^n}} = \frac{D_{ref} - \frac{TD_{50}(1)}{\left(\sum_{j=1}^{M} v_j \left(\frac{D_j}{D_{ref}}\right)^{\frac{1}{n}}\right)^n}}{m \cdot \frac{TD_{50}(1)}{\left(\sum_{j=1}^{M} v_j \left(\frac{D_j}{D_{ref}}\right)^{\frac{1}{n}}\right)^n}} = \frac{1 - \frac{TD_{50}(1)}{\left(\sum_{j=1}^{M} v_j D_j^{\frac{1}{n}}\right)^n}}{m \cdot \frac{TD_{50}(1)}{\left(\sum_{j=1}^{M} v_j D_j^{\frac{1}{n}}\right)^n}} =$$

$$\frac{1 - \frac{TD_{50}(1)}{\mathrm{gEUD}_n(\boldsymbol{D})}}{m \cdot \frac{TD_{50}(1)}{\mathrm{gEUD}_n(\boldsymbol{D})}} = \frac{\mathrm{gEUD}_n(\boldsymbol{D}) - TD_{50}(1)}{m \cdot TD_{50}(1)},$$

which concludes our proof that the LKB model is an NTCP model directly depending on the generalized Equivalent Uniform Dose as defined by [2].

C Inclusion of Relative Biological Effectiveness

Throughout the paper we included RBE effects by using $\mathrm{RBE}_{\mathrm{proton}} = 1.1$ and consequently presenting all proton physical doses as the RBE corrected doses $D_{\mathrm{proton}} = \mathrm{RBE}_{\mathrm{proton}} \tilde{D}_{\mathrm{proton}}$. All BED calculations were done subsequent to taking into account the RBE effect, thus the derived proton doses for new fractionation regiments and new dose shape factors were directly the RBE corrected doses. This is consistent with current clinical practice, where the proton RBE is assumed to be fraction-size independent. In [34] a modified BED formulation is presented that directly incorporates RBE effects into the BED model. This modified BED formulation reads

$$\mathrm{BED} = D\left(\mathrm{RBE} + \frac{D}{N\alpha/\beta_L}\right),$$

where α/β_L is the α/β ratio representative for low Linear Energy Transfer (LET) radiation (practically photons, simply denoted as α/β from this point), and D and RBE are the (non-RBE adjusted) dose and the intrinsic RBE value for the given radiation (which can be both low and high LET). All our results can be generalized according to this Dale-Jones RBE model, and this appendix presents both these general formulas, as well as the sensitivity of our results to this different formulation.

C.1 Generalized BED formulas

Equating the BEDs for two regimens with different radiations yields the general counterpart of Equation 2 as

$$D_{\mathrm{new}}\left(\mathrm{RBE}_{\mathrm{new}} + \frac{D_{\mathrm{new}}}{N_{\mathrm{new}}\alpha/\beta}\right) = D_{\mathrm{ref}}\left(\mathrm{RBE}_{\mathrm{ref}} + \frac{D_{\mathrm{ref}}}{N_{\mathrm{ref}}\alpha/\beta}\right). \quad (14)$$

The solution of Equation 14 for the new dose D_{new} (c.f. Equation 3) is

$$D_{\mathrm{new}} = \frac{1}{2}\left[\sqrt{(N_{\mathrm{new}}\alpha/\beta\mathrm{RBE}_{\mathrm{new}})^2 + 4D_{\mathrm{ref}}\left(N_{\mathrm{new}}\alpha/\beta\mathrm{RBE}_{\mathrm{ref}} + D_{\mathrm{ref}}\frac{N_{\mathrm{new}}}{N_{\mathrm{ref}}}\right)} - N_{\mathrm{new}}\alpha/\beta\mathrm{RBE}_{\mathrm{new}}\right]. \quad (15)$$

The mean BED is a straightforward extension of Equation 4 with the RBE effect leading to

$$\mathrm{BED}_{\mathrm{mean}} = D_{\mathrm{mean}} \left(\mathrm{RBE} + \frac{D_{\mathrm{mean}}}{N\alpha/\beta}\varphi \right). \tag{16}$$

Therefore, a new mean dose tolerance D_{mean} can be obtained in a mean BED equivalent manner by solving

$$D_{\mathrm{new}} \left(\mathrm{RBE}_{\mathrm{new}} + \frac{D_{\mathrm{new}}}{N_{\mathrm{new}}\alpha/\beta}\varphi_{\mathrm{new}} \right) = D_{\mathrm{ref}} \left(\mathrm{RBE}_{\mathrm{ref}} + \frac{D_{\mathrm{ref}}}{N_{\mathrm{ref}}\alpha/\beta}\varphi_{\mathrm{ref}} \right) \tag{17}$$

instead of Equation 6. The solution (c.f. Equation 7) is

$$D_{\mathrm{new}} = \frac{1}{2} \left[\sqrt{\left(\frac{N_{\mathrm{new}}\alpha/\beta \mathrm{RBE}_{\mathrm{new}}}{\varphi_{new}} \right)^2 + 4D_{\mathrm{ref}} \left(\frac{N_{\mathrm{new}}\alpha/\beta \mathrm{RBE}_{\mathrm{ref}}}{\varphi_{\mathrm{new}}} + D_{ref} \frac{\varphi_{\mathrm{ref}}}{\varphi_{\mathrm{new}}} \frac{N_{\mathrm{new}}}{N_{\mathrm{ref}}} \right)} - \frac{N_{\mathrm{new}}\alpha/\beta \mathrm{RBE}_{\mathrm{new}}}{\varphi_{\mathrm{new}}} \right]. \tag{18}$$

Last, the formula for the generalized Equivalent Uniform BED with the RBE being taken into account (c.f. Equation 9) reads

$$\mathrm{gEUBED}_n \left(\boldsymbol{D}, N, \alpha/\beta, \mathrm{RBE} \right) = \frac{1}{M} \left[\sum_{i=1}^{M} \left(D_i \left(\mathrm{RBE} + \frac{D_i}{N\alpha/\beta} \right) \right)^{1/n} \right]^n. \tag{19}$$

Thus, for iso-toxic dose escalation, i.e. to calculate how a dose distribution $\boldsymbol{D}_{\mathrm{new}}$ (with a radiation type having an RBE value $\mathrm{RBE}_{\mathrm{new}}$) can be scaled to a distribution $f \cdot \boldsymbol{D}_{\mathrm{new}}$ such that it leads to the same NTCP as the reference distribution $\boldsymbol{D}_{\mathrm{ref}}$ (with an RBE value of $\mathrm{RBE}_{\mathrm{ref}}$),

$$\mathrm{gEUBED}_n \left(f \cdot \boldsymbol{D}_{\mathrm{new}}, N_{\mathrm{new}}, \alpha/\beta, \mathrm{RBE}_{new} \right) = \mathrm{gEUBED}_n \left(\boldsymbol{D}_{\mathrm{ref}}, N_{\mathrm{ref}}, \alpha/\beta, \mathrm{RBE}_{ref} \right)$$

has to hold, leading to the general counterpart of Equation 10, reading

$$\left[\frac{1}{M} \sum_{i=1}^{M} \left(f \cdot D_{\mathrm{new},i} \left(\mathrm{RBE}_{\mathrm{new}} + \frac{f \cdot D_{\mathrm{new},i}}{N_{\mathrm{new}}\alpha/\beta} \right) \right)^{1/n} \right]^n = \left[\frac{1}{M} \sum_{i=1}^{M} \left(D_{\mathrm{ref},i} \left(\mathrm{RBE}_{\mathrm{ref}} + \frac{D_{\mathrm{ref},i}}{N_{\mathrm{ref}}\alpha/\beta} \right) \right)^{1/n} \right]^n. \tag{20}$$

This more consistent formulation decreases the BED values for all proton plans. In our original formulation, the proton physical doses $D_{\mathrm{proton}} = \mathrm{RBE}_{\mathrm{proton}} \tilde{D}_{\mathrm{proton}}$ were used directly in the BED equation, leading to $\mathrm{BED} = D_{\mathrm{proton}} \left(1 + \frac{D_{\mathrm{proton}}}{N\alpha/\beta} \right)$. In contrast, the more consistent formulation reads $\tilde{D}_{\mathrm{proton}} \left(\mathrm{RBE}_{\mathrm{proton}} + \frac{\tilde{D}_{\mathrm{proton}}}{N\alpha/\beta} \right) = D_{\mathrm{proton}} \left(1 + \frac{D_{\mathrm{proton}}}{N\alpha/\beta \mathrm{RBE}^2_{\mathrm{proton}}} \right)$, obviously smaller for RBE values above 1. The relative BED difference (compared to our original formulation) is

$$\frac{\Delta\mathrm{BED}}{\mathrm{BED}} = -\frac{\mathrm{RBE}^2_{\mathrm{proton}} - 1}{\mathrm{RBE}^2_{\mathrm{proton}}} \frac{1}{1 + \frac{N\alpha/\beta}{D_{\mathrm{proton}}}}. \tag{21}$$

For $\mathrm{RBE}_{\mathrm{proton}} = 1.1$ this translates to a maximum difference of -17.3% (for $D_{\mathrm{proton}}/N = \infty$), and it decreases with decreasing dose per fraction size (e.g. for $D_{\mathrm{proton}}/N = 2\,\mathrm{Gy}$ and $\alpha/\beta = 3\,\mathrm{Gy}$ we find $\Delta\mathrm{BED}/\mathrm{BED} = -6.9\%$).

C.2 Sensitivity to Accounting for RBE

To test the sensitivity of our results to the different incorporation of the RBE all calculations have been done using both approaches. Figure 7 shows the general counterparts of the most important figures regarding the shape and fractionation effects, displaying both the results of our original formulation (labeled as "Constant RBE" in blue) as well as the formulation of [34] ("Dale-Jones RBE" in red). As expected, the more consistent methodology decreases effects. Nevertheless, the differences are small

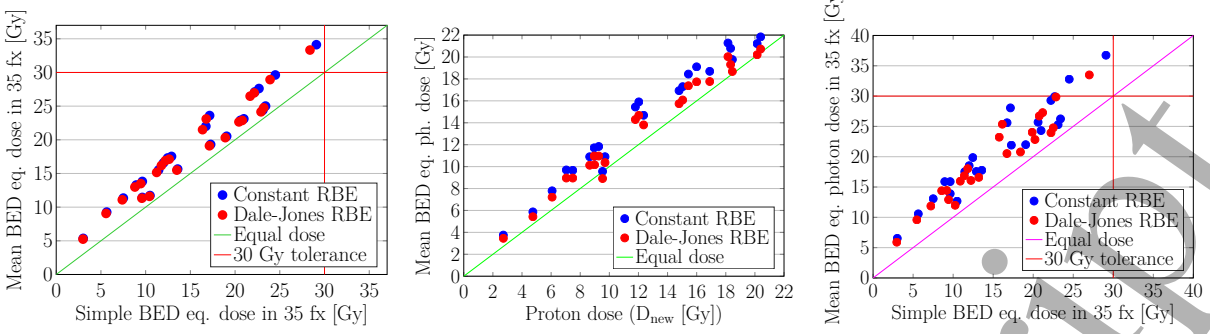

(a) Mean doses in 35 fractions that are equivalent with the given proton doses in 5/15 fractions, with (y-axis) and without (x-axis) taking into account the dose shape (c.f. Figure 2b).

(b) Mean BED equivalent photon mean dose as a function of proton mean dose (c.f. Figure 4c).

(c) Mean BED equivalent 35-fraction photon mean doses versus simple BED equivalent 35-fraction mean doses (c.f. Figure 5).

Figure 7. The influence of the method of taking into account the RBE of protons. The Dale-Jones RBE model predicts slightly smaller effects than the constant RBE method, however the differences do not alter our main conclusions.

(around 5-10%), and our main conclusions remain valid: neglecting the shape effect when calculating iso-effective doses in new fractionation schemes (Figure 7a) and new modalities (Figure 7b) underestimates their biological effects, and there are situations where neglecting the dose shape effect leads to significantly lower doses than are iso-effective (Figure 7c).

The effect of the proton RBE incorporation on the dose escalation potential of protons compared to photons is also relatively small (see Figure 8). All physical dose based results ($\alpha/\beta = \infty$) naturally remain unchanged, whereas the BED based calculations ($\alpha/\beta < \infty$) yield around 5-10% higher proton/photon GTV dose ratios than our original formulation (compare with Figure 6). This is a straightforward consequence of the different handling of the RBE: since the Dale-Jones method leads to lower BED values for protons, photon doses - for which the 2 formulations are identical - can be scaled less, leading to higher proton/photon target dose ratios. For a mean BED constraint ($n = 1$) with our hypofractionated (5/15 fraction) treatments adjusting for fractionation decreases protons' dose escalation potential to only 12% compared to the 25% based on physical dose, and for $n = 1.1$ [35] to only 17% compared to 35% (c.f. our 5% and 10% estimates based on Figure 6a). Just as is the case in Section 3.5, the differences somewhat decrease when standard fractionation is assumed (Figure 8b). Understandably, the biggest contrast between the two formulations is seen for $n \in [0, 0.6]$, since for small volume parameters more and more the highest dose values matter (i.e. the voxels having the highest doses and dose per fraction values), and the BED difference is increasing with the dose per fraction (in accordance with Equation 21). In this region the BED adjustment including RBE predicts higher dose escalation potential than based on physical dose, as the degradation due to accounting for fractionation is counterbalanced by the more beneficial RBE effect. For $n > 0.6$ the fractionation effect becomes dominant (as all voxels become increasingly important), and though the Dale-Jones RBE approach does predict a higher dose escalation potential for protons than our constant RBE approach, this potential is still substantially lower than is expected based on physical dose.

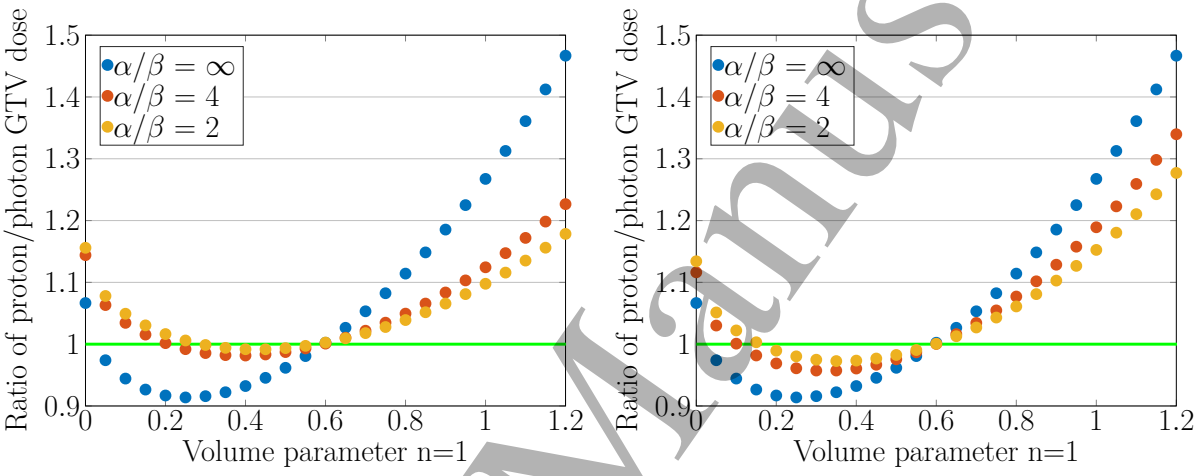

(a) Reference: hypofractionated (5/15 fraction), clinically delivered proton plans (c.f. Figure 6a).

(b) Reference: scaled proton plans assuming standard fractionation (70 Gy GTV dose with 2 Gy/fx, 35 fractions, c.f. Figure 6b).

Figure 8. Dose escalation potential of protons vs. photons for equivalent gEUD based NTCP values with various volume parameters n and fractionation sensitivities α/β, with the Dale-Jones method of accounting for RBE based on [34].

References

[1] Andrzej Niemierko. Reporting and analyzing dose distributions: a concept of equivalent uniform dose. *Medical physics*, 24(1):103–110, 1997.

[2] Andrzej Niemierko. A generalized concept of equivalent uniform dose (EUD). *Medical Physics*, 26:1100 (abstract), 1999.

[3] Beong Choi and Joseph O. Deasy. The generalized equivalent uniform dose function as a basis for intensity-modulated treatment planning. *Physics in Medicine and Biology*, 47(20):3579–3589, oct 2002.

[4] Søren M. Bentzen, Matthew Parliament, Joseph O. Deasy, Adam Dicker, Walter J. Curran, Jacqueline P. Williams, and Barry S. Rosenstein. Biomarkers and Surrogate Endpoints for Normal-Tissue Effects of Radiation Therapy: The Importance of Dose-Volume Effects. *International Journal of Radiation Oncology Biology Physics*, 76(3 SUPPL.):145–150, 2010.

[5] B Emami. Tolerance of Normal Tissue to Therapeutic Radiation. *Reports of Radiotherapy and Oncology*, 1(1):36–48, 2013.

[6] Jacques Bernier, Eric J Hall, and Amato Giaccia. Radiation oncology: a century of achievements. *Nature reviews. Cancer*, 4(9):737–747, 2004.

[7] L. Moonen and H Bartelink. Fractionation in radiotherapy. *Cancer Treatment Reviews*, 20(4):365–378, oct 1994.

[8] J F Fowler. What next in fractionated radiotherapy? *The British journal of cancer*, 49(Supplement VI.):285–300, 1984.

[9] H R Withers. Biologic basis for altered fractionation schemes. *Cancer*, 55(9 Suppl):2086–2095, 1985.

[10] B G Douglas and J F Fowler. The Effect of Multiple Small Doses of X Rays on Skin Reactions in the Mouse and a Basic Interpretation. *Radiation research*, 66(2):401–426, 1976.

[11] Henri Coutard. Principles of x ray therapy of malignant diseases. *The Lancet*, 224(5784):1–8, 1934.

[12] Bridget F. Koontz, Alberto Bossi, Cesare Cozzarini, Thomas Wiegel, and Anthony D'Amico. A systematic review of hypofractionation for primary management of prostate cancer. *European Urology*, 68(4):683–691, 2015.

[13] Chad G. Rusthoven, Christine F. Lauro, Brian D. Kavanagh, and Tracey E. Schefter. Stereotactic body radiation therapy (SBRT) for liver metastases: A clinical review. *Seminars in Colon and Rectal Surgery*, 25(1):48–52, 2014.

[14] C Armpilia, C Antypas, A Zygogianni, M Balafouta, P Sandilos, and J Kouvaris. A review on radiotherapy hypofractionation schedules for breast cancer treatment. *Journal of Radiotherapy in Practice*, 10(3):201–208, 2011.

[15] I Beli, G Koukourakis, K Platoni, M Tolia, N Kelekis, J Kouvaris, C Syrigos, K Mystakidou, C Varveris, and V Kouloulias. Hypofractionated radiotherapy in non small cell lung cancer: a review of the current literature. *Reviews on recent clinical trials*, 5(2):103–11, 2010.

[16] Jack F. Fowler. 21 Years of biologically effective dose. *British Journal of Radiology*, 83(991):554–568, 2010.

[17] G. W. Barendsen. Dose fractionation, dose rate and iso-effect relationships for normal tissue responses. *International Journal of Radiation Oncology, Biology, Physics*, 8(11):1981–1997, 1982.

[18] Aswin L Hoffmann and Alan E Nahum. Fractionation in normal tissues: the (α/β)eff concept can account for dose heterogeneity and volume effects. *Physics in medicine and biology*, 58(19):6897–914, 2013.

[19] Board of the Faculty of Clinical Oncology (The Royal College of Radiologists). The timely delivery of radical radiotherapy : standards and guidelines for the management of unscheduled treatment interruptions , Third edition. Technical report, Royal College of Radiologists, 2008.

[20] C. H. Newcomb, J. Van Dyk, and R. P. Hill. Evaluation of isoeffect formulae for predicting radiation-induced lung damage. *Radiotherapy and Oncology*, 26(1):51–63, 1993.

[21] H. Rodney Withers, Howard D. Thames, and Lester J. Peters. A new isoeffect curve for change in dose per fraction. *Radiotherapy and Oncology*, 1(2):187–191, nov 1983.

[22] An Tai, Beth Erickson, and X. Allen Li. Extrapolation of Normal Tissue Complication Probability For Different Fractionations in Liver Irradiation. *International Journal of Radiation Oncology Biology Physics*, 74(1):283–289, 2009.

[23] Charlie C. Pan, Brian D. Kavanagh, Laura A. Dawson, X. Allan Li, Shiva K. Das, Moyed Miften, and Randall K. Ten Haken. Radiation-Associated Liver Injury. *International Journal of Radiation Oncology Biology Physics*, 76(3):94–100, 2010.

[24] Lawrence B. Marks, Soren M. Bentzen, Joseph O. Deasy, Feng-Ming (Spring) Kong, Jeffrey D. Bradley, Ivan S. Vogelius, Issam El Naqa, Jessica L. Hubbs, Joos V. Lebesque, Robert D. Timmerman, Mary K. Martel, and Andrew Jackson. Radiation Dose-Volume Effects in the Lung. *International Journal of Radiation Oncology*Biology*Physics*, 76(3):S70–S76, 2010.

[25] Sarah C Darby, Marianne Ewertz, Paul McGale, Anna M Bennet, Ulla Blom-Goldman, Dorthe Brønnum, Candace Correa, David Cutter, Giovanna Gagliardi, Bruna Gigante, Maj-Britt Jensen, Andrew Nisbet, Richard Peto, Kazem Rahimi, Carolyn Taylor, and Per Hall. Risk of ischemic heart disease in women after radiotherapy for breast cancer. *The New England journal of medicine*, 368(11):987–98, 2013.

[26] Theodore Hong. A Phase II Randomized Trial of IMPT vs. IMRT for Hepatocellular Carcinoma. Technical report, Massachusetts General Hospital, Boston, 2016.

[27] Harald Paganetti. *Proton Therapy Physics*. CRC Press, Inc., New York, 2012.

[28] Lawrence B. Marks, Randall K. Ten Haken, and Mary K. Martel. Guest Editor's Introduction to QUANTEC: A Users Guide. *International Journal of Radiation Oncology Biology Physics*, 76(3 SUPPL.):2009–2010, 2010.

[29] G J Kutcher and C Burman. Calculation of complication probability factors for non-uniform normal tissue irradiation: the effective volume method. *International journal of radiation oncology, biology, physics*, 16(6):1623–1630, 1989.

[30] Lawerence B Marks, Ellen D Yorke, Andrew Jackson, Randall K Ten Haken, Louis S Constine, Joseph O Deasy, Jiho Nam, Avraham Eisbruch, and Søren M Bentzen. Models in the Clinic. *International journal radiation oncology.*, 76(3 0):1–17, 2010.

[31] Laura A. Dawson, Daniel Normolle, James M. Balter, Cornelius J. McGinn, Theodore S. Lawrence, and Randall K. Ten Haken. Analysis of radiation-induced liver disease using the Lyman NTCP model. *International Journal of Radiation Oncology Biology Physics*, 53(4):810–821, 2002.

[32] Alan E. Nahum. The Radiobiology of Hypofractionation. *Clinical Oncology*, 27(5):260–269, 2015.

[33] Aswin L Hoffmann, Dick den Hertog, Alex Y D Siem, Johannes H a M Kaanders, and Henk Huizenga. Convex reformulation of biologically-based multi-criteria intensity-modulated radiation therapy optimization including fractionation effects. *Physics in Medicine and Biology*, 53(22):6345–6362, nov 2008.

[34] Roger G. Dale and Bleddyn Jones. The assessment of RBE effects using the concept of biologically effective dose. *International Journal of Radiation Oncology Biology Physics*, 43(3):639–645, 1999.

[35] Laura A. Dawson and James M. Balter. Interventions to Reduce Organ Motion Effects in Radiation Delivery. *Seminars in Radiation Oncology*, 14(1):76–80, 2004.

[36] Yvette Seppenwoolde, Joos V. Lebesque, Katrien De Jaeger, José S a Belderbos, Liesbeth J. Boersma, Cees Schilstra, George T. Henning, James a. Hayman, Mary K. Martel, and Randall K. Ten Haken. Comparing different NTCP models that predict the incidence of radiation pneumonitis. *International Journal of Radiation Oncology Biology Physics*, 55(3):724–735, 2003.

[37] Laura a Dawson, Cynthia Eccles, and Tim Craig. Individualized image guided iso-NTCP based liver cancer SBRT. *Acta oncologica (Stockholm, Sweden)*, 45(7):856–864, 2006.

[38] Wei-Xiang Qi, Shen Fu, Qing Zhang, and Xiao-Mao Guo. Charged particle therapy versus photon therapy for patients with hepatocellular carcinoma: A systematic review and meta-analysis. *Radiotherapy and Oncology*, 114(3):289–295, 2015.

[39] Robert D. Timmerman. An Overview of Hypofractionation and Introduction to This Issue of Seminars in Radiation Oncology. *Seminars in Radiation Oncology*, 18(4):215–222, 2008.

[40] David J. Brenner. The Linear-Quadratic Model Is an Appropriate Methodology for Determining Isoeffective Doses at Large Doses Per Fraction. *Seminars in Radiation Oncology*, 18(4):234–239, 2008.

[41] John P. Kirkpatrick, Jeffrey J. Meyer, and Lawrence B. Marks. The Linear-Quadratic Model Is Inappropriate to Model High Dose per Fraction Effects in Radiosurgery. *Seminars in Radiation Oncology*, 18(4):240–243, 2008.

[42] Pierre Blanchard, Andrew J. Wong, G. Brandon Gunn, Adam S. Garden, Abdallah S.R. Mohamed, David I. Rosenthal, Joseph Crutison, Richard Wu, Xiaodong Zhang, X. Ronald Zhu, Radhe Mohan, Mayankkumar V. Amin, C. David Fuller, and Steven J. Frank. Toward a model-based patient selection strategy for proton therapy: External validation of photon-derived normal tissue complication probability models in a head and neck proton therapy cohort. *Radiotherapy and Oncology*, 121(3):381–386, dec 2016.

[43] Johannes A. Langendijk, Philippe Lambin, Dirk De Ruysscher, Joachim Widder, Mike Bos, and Marcel Verheij. Selection of patients for radiotherapy with protons aiming at reduction of side effects: The model-based approach. *Radiotherapy and Oncology*, 107(3):267–273, 2013.

[44] Stefan L S Kwa, Jacqueline C M Theuws, Antoinette Wagenaar, Eugene M F Damen, Liesbeth J Boersma, Paul Baas, Sara H Muller, and Joos V Lebesque. Evaluation of two dose - volume histogram reduction models for the prediction of radiation pneumonitis. *Science*, 48:61–69, 1998.

[45] Jose Belderbos, Wilma Heemsbergen, Mischa Hoogeman, Kenneth Pengel, Maddalena Rossi, and Joos Lebesque. Acute esophageal toxicity in non-small cell lung cancer patients after high dose conformal radiotherapy. *Radiotherapy and Oncology*, 75(2):157–164, 2005.

[46] Olivier Chapet, Feng Ming Kong, Julia S. Lee, James A. Hayman, and Randall K. Ten Haken. Normal tissue complication probability modeling for acute esophagitis in patients treated with conformal radiation therapy for non-small cell lung cancer. *Radiotherapy and Oncology*, 77(2):176–181, 2005.

[47] T. Rancati, C. Fiorino, G. Gagliardi, G. M. Cattaneo, G. Sanguineti, V. Casanova Borca, C. Cozzarini, G. Fellin, F. Foppiano, G. Girelli, L. Menegotti, A. Piazzolla, V. Vavassori, and R. Valdagni. Fitting late rectal bleeding data using different NTCP models: Results from an Italian multi-centric study (AIROPROS0101). *Radiotherapy and Oncology*, 73(1):21–32, 2004.

[48] Hiram A. Gay and Andrzej Niemierko. A free program for calculating EUD-based NTCP and TCP in external beam radiotherapy. *Physica Medica*, 23(3-4):115–125, 2007.

[49] Wolfgang A. Tomé and John D. Fenwick. Analysis of radiation-induced liver disease using the lyman ntcp model: in regard to Dawson et al. ijrobp 2002;53:810-821. *International Journal of Radiation Oncology*Biology*Physics*, 58(4):1318–1319, mar 2004.

[50] Søren M. Bentzen, Wolfgang Dörr, Reinhard Gahbauer, Roger W. Howell, Michael C. Joiner, Bleddyn Jones, Dan T L Jones, Albert J. Van Der Kogel, André Wambersie, and Gordon Whitmore. Bioeffect modeling and equieffective dose concepts in radiation oncology-Terminology, quantities and units. *Radiotherapy and Oncology*, 105(2):266–268, 2012.

[51] John C. Flickinger and Andre Kalend. Use of normalized total dose to represent the biological effect of fractionated radiotherapy. *Radiotherapy and Oncology*, 17(4):339–347, apr 1990.

[52] Joos V. Lebesque and Ronald B. Keus. The simultaneous boost technique: the concept of relative normalized total dose. *Radiotherapy and Oncology*, 22(1):45–55, 1991.

[53] Clinton S. Park, Yongbok Kim, Nancy Lee, Kara M. Bucci, Jeanne M. Quivey, Lynn J. Verhey, and Ping Xia. Method to account for dose fractionation in analysis of IMRT plans: Modified equivalent uniform dose. *International Journal of Radiation Oncology Biology Physics*, 62(3):925–932, 2005.

[54] Gary Luxton, Paul J Keall, and Christopher R King. A new formula for normal tissue complication probability (NTCP) as a function of equivalent uniform dose (EUD). *Physics in Medicine and Biology*, 53(1):23–36, jan 2008.

[55] Therapy Physics Committee AAPM Task Group 166. The Use and QA of Biologically Related Models for Treatment Planning. Technical Report 166, AAPM Task Group 166 of the Therapy Physics Committee, 2012.

[56] J T Lyman. Complication probability as assessed from dose-volume histograms. *Radiation research. Supplement*, 8:S13–S19, 1985.